Journal of ELECTRONIC MATERIALS, Vol. 49, No. 1, 2020
https://doi.org/10.1007/s11664-019-07795-2

Enhanced Thermoelectric Performance of *n*-Type Polycrystalline SnSe via $MoCl_5$ Doping

TONG SHEN,[1] KANG YIN LI,[1] ZI JIE CHEN,[1] HAI FEI WU,[2] and JIAN XIAO SI [1,3]

1.—Department of Physics, Zhejiang Normal University, Jinhua 321004, People's Republic of China. 2.—Department of Physics, Shaoxing University, Shaoxing 312000, People's Republic of China. 3.—e-mail: sjx@zjnu.cn

n-Type polycrystalline $SnSe_{0.95}$-*x*%$MoCl_5$ (*x* = 0.5, 1.0, 1.5, 2) samples have been synthesized by melting and hot-pressing. The effect of $MoCl_5$ doping on thermoelectric properties is investigated. The multipoint defects of Cl_{se} and Mo_{sn} increased the carrier concentration from 5.3×10^{17} cm^{-3} (*p*-type) in undoped SnSe to 1.76×10^{19} cm^{-3} (*n*-type) in $SnSe_{0.95}$-1.5%$MoCl_5$ sample, which leads to increased electrical conductivity. Moreover, the multipoint defects enhanced the phonon scattering and resulted in a suppression of the thermal conductivity. As a result, a peak value *ZT* of 0.66 was obtained at 773 K for $SnSe_{0.95}$-1%$MoCl_5$. These results show that $MoCl_5$ could be an effective dopant for improving the thermoelectric performance of *n*-type SnSe.

Key words: Polycrystalline SnSe, *n*-type, Thermoelectric, $MoCl_5$

INTRODUCTION

Thermoelectric (TE) materials, which can directly and reversibly convert heat energy into electrical power have attracted significant interest to satisfy energy demands.[1,2] The performance of thermoelectric materials is characterized by the dimensionless figure of merit $ZT = S^2\sigma T/\kappa$, where *S* is the Seebeck coefficient, σ is the electrical conductivity, κ is the thermal conductivity and *T* is the absolute temperature.[3,4] Excellent thermoelectric materials should possess high power factor ($S^2\sigma$) and low thermal conductivity (κ) simultaneously. However, due to the complex interrelationships among the parameters, it is still a challenge to decouple these parameters to achieve a high *ZT*. a successful strategy to achieve a high *ZT* is to seek materials with intrinsic low thermal conductivity.[5]

Tin selenide (SnSe), consisting of earth-abundant and low-toxicity elements, has been found to exhibit ultrahigh *ZT* of ≈ 2.6 (*p*-type) at 923 K and ≈ 2.8(*n*-type) at 773 K in single crystals owing to low thermal conductivity along specified crystallographic directions.[6,7] However, the difficulties in synthesis, high cost and poor machinability of single crystals limit their mass production and broad-based application. Thus, considerable effort has been focused on improving the thermoelectric performance of polycrystalline SnSe.[8] Recently, a record-high *ZT* of 2.5 at 773 K for *p*-type polycrystalline SnSe has been achieved using oxide removal.[9] In contrast, the *n*-type polycrystalline SnSe still exhibits much inferior performance because of its intrinsic *p*-type conducting behavior. It is difficult to tune an *n*-type charge carrier at an optimal level due to a large amount of Sn vacancies. Doping with Bi for cationic substitution has been proven to be invalid to increase electron carrier concentration and a low *ZT* value of 0.025 at 723 K was obtained in the SnSe:Bi 8% sample.[10] The transition metal Ti as cation-site doping was used to realize *n*-type doping and a slightly improved TE performance (*ZT* ≈ 0.4)is achieved at 773 K for the sample $Sn_{0.74}Pb_{0.20}Ti_{0.06}Se$.[11] Halogens, such as Cl, Br, and I with anion-site doping, were found to be effective for the preparation of *n*-type SnSe.[5,12,13] A *ZT* of 0.8 at 773 K was obtained in $SnSe_{0.96}I_{0.04}$ with low electron carrier concentration ≈ 2.0×10^{17} cm^{-3}. When Cl was used as *n*-type dopant in

(Received September 11, 2019; accepted October 31, 2019; published online November 12, 2019)

$SnSe_{0.95}Cl_{0.05}$ sample, the electron carrier concentration could be increased to $\approx 4.5 \times 10^{18}$ cm^{-3},[12] while an improved ZT of ≈ 1.3 at 773 K was achieved with a high electron concentration of $\approx 9.3 \times 10^{18}$ cm^{-3} via heavy Br doping.[5] A more effective way to enhance ZT in n-type polycrystalline SnSe is to introduce cationic and anionic substitution at Sn and Se sites simultaneously by a multiple-step doping process or co-doping approach.[12,14,15] Wang et al. reported that the $BiCl_3$ doping significantly increased the carrier concentration up to 1.5×10^{19} cm^{-3} leading to an enhancement of electrical conductivity and a ZT of 0.7 at 793 K[14]. Pb and Br or Pb and Cl co-doped n-type SnSe samples have been reported with a ZT range from ~0.5 to ~1.2.[12,15] The highest of ZT value (1.5 at 798 K) for n-type polycrystalline SnSe was obtained in $Sn_{1-x}Re_xSe_{0.93}Cl_{0.02}$ samples using multipoint defect synergy, which demonstrated that transition-metal elements coupled with Cl may be effective dopants for point defect engineering.[16] This motivates us to find whether the transition metal chlorides are applicable in enhancing the thermoelectric properties of n-type polycrystalline SnSe.

In this work, we choose $MoCl_5$ as a new dopant with a lower melting point than that of Mo to enhance the TE performance of n-type polycrystalline SnSe. A series of polycrystalline $SnSe_{0.95}$-x%$MoCl_5$ (x = 0, 0.5, 1.0, 1.5, 2) samples have been synthesized by melting and hot-pressing. The $MoCl_5$ doping simultaneously introduced Cl_{se} and Mo_{sn} defects in SnSe, which contribute to enhancing electrical conductivity and reducing thermal conductivity concurrently. A peak value ZT of 0.66 was obtained at 773 K for $SnSe_{0.95}$-1%$MoCl_5$.These results show that $MoCl_5$ could be an effective dopant for improving the thermoelectric performances of n-type SnSe.

EXPERIMENTAL

High-purity raw materials, Sn (99.95%, Alfa Aesar), Se (99.95% Alfa Aesar) and $MoCl_5$(99%, Alfa Aesar) were weighed according to the stoichiometric ratio of $SnSe_{0.95}$-x%$MoCl_5$(x = 0, 0.5, 1, 1.5, 2) and sealed into evacuated quartz tubes under high vacuum (< 10^{-3} Pa). The tubes were heated up to 1127 K at a rate of 600 K $h^{-1}$and kept at that temperature for 2 h, then slowly cooled down to 873 K at a rate of 70 K h^{-1} and kept 3 h, after which they were slowly cooled down to room temperature. The obtained ingots were ground into powders and were loaded in a graphite die and hot pressed under an axial pressure of 50 MPa for 10 min at 773 K in a vacuum.

The phase structure was identified by powder X-ray diffraction (XRD) (Bruker D8, Cu-Kα). The morphology and elemental distribution mapping of samples were examined using a field emission scanning microscope (FESEM, Hitachi, S-4800). The Seebeck coefficient and electrical conductivity were measured simultaneously using a commercial system (CTA-3) from room temperature to 773 K in a helium atmosphere. The Hall coefficient was tested by Van der Pauw technique with an HMS-3000 system. The thermal conductivity was determined by the relationship $\kappa = DC_P\lambda$ where D is volumetric density measured using the Archimedes principle, C_p is specific heat capacity taken from previous data,[4,15] and λ is thermal diffusivity measured using a laser-flash system (LFA467, Linseis). The uncertainty is 5% for the Seebeck coefficient, 4% for the electrical conductivity and 10% for the thermal conductivity. Therefore, the combined uncertainty for the experimental measurements of ZT was estimated to be about 15%.

RESULTS AND DISCUSSION

Figure 1a shows the XRD patterns of all the $SnSe_{0.95}$-x%$MoCl_5$ (x = 0, 0.5, 1, 1.5, 2) samples measured perpendicular to the pressure direction. The patterns can be indexed to the orthorhombic SnSe phase (PDF#48-1224) as the major phase in all samples, besides the trace amount of Sn (JCPDS no.04–0673) observed, labeled by diamond. Furthermore, the impurity phase of $MoSe_2$ marked by an asterisk is detected up to x = 1, as shown in Fig. 1a. The existence of a $MoSe_2$ phase suggests that the solubility limit of $MoCl_5$ in SnSe is less than 1 at.% under the situation of rich Sn. The inset of Fig. 1a shows an enlarged view of XRD in the range of 30-33^0, which shows that the diffraction peak shifted toward lower angles as the $MoCl_5$ content increased. The expansion of the lattice in $SnSe_{0.95}$-x%$MoCl_5$ samples is mainly because of the larger ionic radius of Mo (1.36 Å) than that of Sn (1.22 Å).[10,17] The calculated lattice parameters as a function of $MoCl_5$ content are shown in Fig. 1b. The lattice parameters of $SnSe_{0.95}$ (a = 11.48 Å, b = 4.15 Å, and c = 4.43 Å) are similar to previously reported values.[6,18] With increasing $MoCl_5$ concentration, the lattice parameter of a increases gradually. In comparison, lattice parameters b and c exhibit a non-monotonic trends as a function of $MoCl_5$ content, which may result from the substitution of the smaller atomic radius of Cl (1.81 Å) into the Se (1.98 Å) sites that shrink the lattice along the bc-plane with strong covalent bonding.[19]

Figure 2a shows the FESEM image of the freshly fractured surface of $SnSe_{0.95}$-1.5%$MoCl_5$ sample. The obvious layered structures with sizes of several microns are observed, indicating an obvious anisotropy in the sintered pellets. Figure 2b shows the polished surface of $SnSe_{0.95}$-1.5%$MoCl_5$ sample and the corresponding EDS maps of Sn, Se, Mo, and Cl are presented in Fig. 2c–f. The results indicated the elements of Sn, Se, Mo, and Cl are all distributed homogeneously. On the basis of the results mentioned above, $MoCl_5$ was successfully incorporated into the Sn and Se lattices.

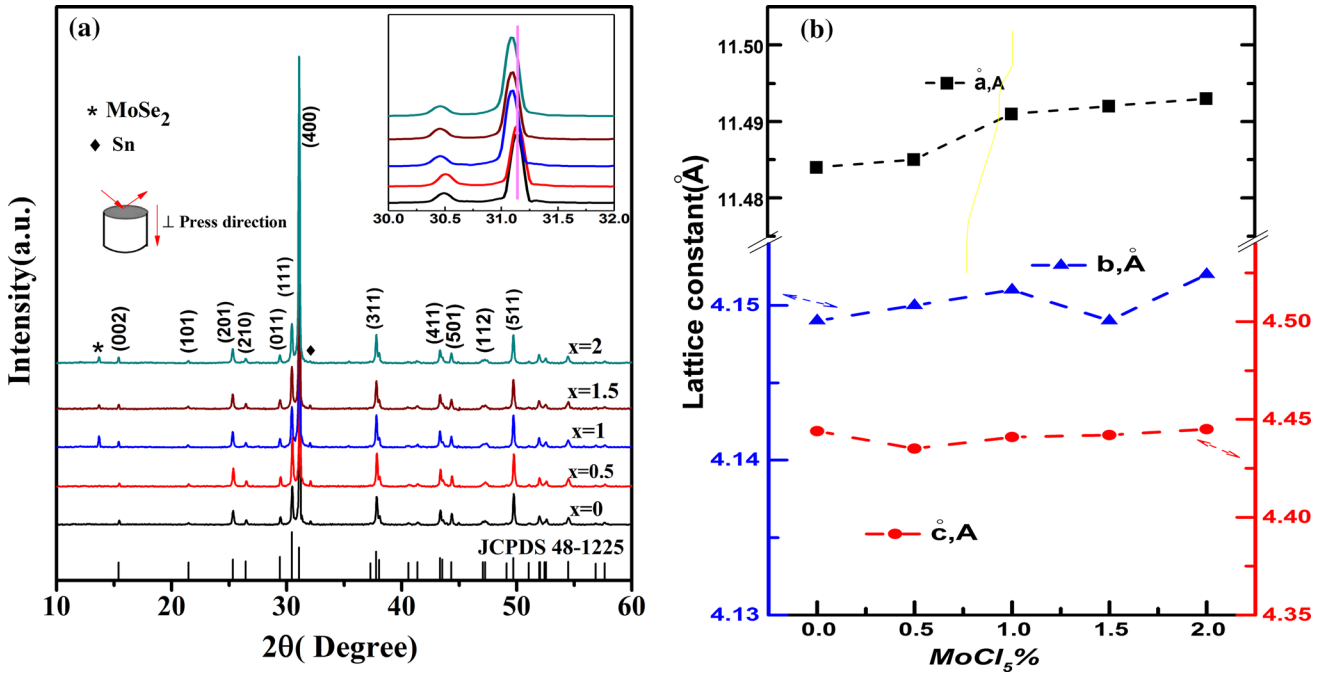

Fig. 1. (a) Powder x-ray diffraction patterns and (b) calculated lattice parameters of the $SnSe_{0.95}$-x%$MoCl_5$ (x = 0, 0.5, 1, 1.5, 2) samples measured perpendicular to the pressure direction. The inset shows enlarged peaks of (111) and (400) peaks to see the deviation.

Figure 3a shows the temperature dependence of the electrical conductivity for the $SnSe_{0.95}$-x%$MoCl_5$ (x = 0, 0.5, 1, 1.5, 2) samples, which were measured perpendicular to the pressing direction. In undoped $SnSe_{0.95}$ the, the electrical conductivity is 0.2 Scm^{-1} at room temperature and increases to 5 Scm^{-1} at 773 K, showing a typical semiconductor behavior, which is similar to a previous report.[5,20] After $MoCl_5$ doping, the electrical conductivity is greatly enhanced compared with the undoped SnSe and sharply increase in the range of 523 K to 673 K. A maximum electrical conductivity of 28 Scm^{-1} is obtained for $SnSe_{0.95}$-1%$MoCl_5$ sample at 673 K. The enhanced electrical conductivity can be attributed to the increased carrier concentration from $MoCl_5$ doping. As shown in Table I, the carrier concentration is monotonically increased from 5.3×10^{17} cm^{-3} for x = 0 to 1.76×10^{19} cm^{-3} for x = 1.5 at 300 K, which is nearly two orders of magnitude higher than that of the undoped sample. Mo substituting Sn and the Cl substituting Se both increase the electron concentrations and the carrier concentration is similar to those reported in $BiCl_3$ dopant sample.[13] It indicates that $MoCl_5$ is an effective dopant in optimizing the carrier concentration for n-type SnSe.

Figure 3b presents the Seebeck coefficients of the $SnSe_{0.95}$-x%$MoCl_5$ (x = 0, 0.5, 1, 1.5, 2) samples as function of temperature. The Seebeck coefficient is positive for undoped SnSe, indicating a p-type semiconductor. After introducing $MoCl_5$, the samples show negative Seebeck coefficients in the whole measured temperature range, which is in agreement with the Hall measurement. The Seebeck coefficient increases from − 110 uV/K at 323 K to − 368 uV/K at 773 K for $SnSe_{0.95}$-1%$MoCl_5$ sample. The Seebeck coefficient shows a near-independent behavior on the amount of $MoCl_5$ above the 573 K, which is consistent with results of Br-doped n-type polycrystalline $SnSe_{1-x}Br_x$ samples with the carrier concentration of 10^{18} cm^{-3}.[5] A possible explanation for the independent behavior is the existence of more pronounced continuous phase transition in n-type SnSe.[7] The dynamic structural behavior of phase transition may lead to a higher symmetry of crystal structure in n-type SnSe and cause a highly anisotropic distribution of charge density due to significant orbital overlap along the out-of-plane direction.

Benefiting from the enhanced electrical conductivity and moderate Seebeck coefficient, the $SnSe_{0.95}$-x%$MoCl_5$ (x = 0, 0.5, 1, 1.5, 2) samples exhibited improvement in power factors, as shown in Fig. 3c. A maximum value of 3.41 $\mu W\ cm^{-1}\ K^{-2}$ at 723 K is obtained for the 1%$MoCl_5$-doped $SnSe_{0.95}$ sample, which was an order of magnitude higher than that of $SnSe_{0.95}$ sample.

Figure 3d shows the total thermal conductivity (κ_{tot}) as a function of temperature for the $SnSe_{0.95}$-x%$MoCl_5$ (x = 0, 0.5, 1, 1.5, 2) samples. The thermal conductivity (κ_{tot}) of $SnSe_{0.95}$ sample is 1.18 $W\ m^{-1}\ K^{-1}$ at 323 K and decreases down to 0.45 $W\ m^{-1}\ K^{-1}$ at 773 K. After doping with $MoCl_5$, the total thermal conductivity (κ_{tot}) of $SnSe_{0.95}$-1%$MoCl_5$ sample is 0.92 $W\ m^{-1}\ K^{-1}$ at 323 K and it reaches the lowest value of 0.38 $W\ m^{-1}\ K^{-1}$ at 773 K. This low thermal conductivity is comparable to the value of 0.38 $W\ m^{-1}\ K^{-1}$ for

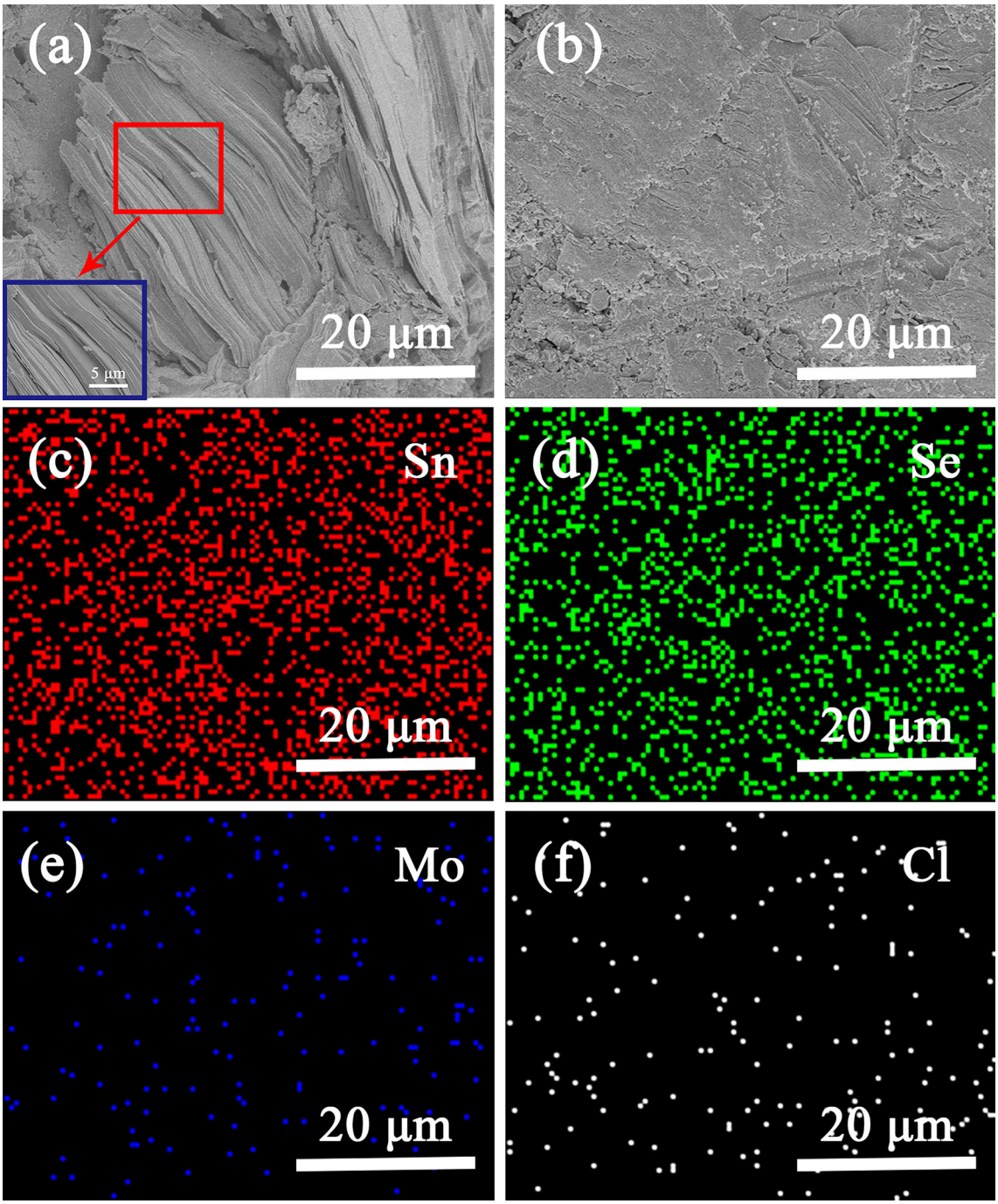

Fig. 2. (a) fractured, (b) polished surface morphologies and EDS mapping of (c) Sn, (d) Se, (e) Mo, (f) Cl of $SnSe_{0.95}$-1.5%$MoCl_5$ sample.

$Sn_{0.97}Re_{0.03}Se_{0.93}Cl_{0.02}$ at 798 K.[16] The lattice thermal conductivity is calculated by using the formula $\kappa_{lat} = \kappa_{tot} - \kappa_{ele}$. The κ_{ele} is obtained via $\kappa_{ele} = L\sigma T$ by the Wiedemann–Franz law. Where σ is the electrical conductivity, T is the absolute temperature and L is the Lorenz number ($\sim 1.5 \times 10^{-8}$ V^2 K^{-2}) obtained by fitting the Seebeck data to the reduced chemical potential.[6,15] Because of poor electrical conductivity, the lattice thermal conductivity is almost the same as total thermal conductivity, as the inset of Fig. 3d shows. The decrease of lattice thermal conductivity for $SnSe_{0.95}$-1%$MoCl_5$ could be attributed to the better phonon scattering by point defects. When $MoCl_5$ doped content is higher than 1%, the thermal conductivity increased, which is attributed to the presence of the $MoSe_2$ with high thermal conductivity as shown in the XRD result.

Figure 3e displays the temperature dependence of ZT values for the $SnSe_{0.95}$-x%$MoCl_5$ (x = 0, 0.5, 1.0, 1.5, and 2) samples. The maximum ZT value of $\sim$ 0.66 was obtained in the $SnSe_{0.95}$-1%$MoCl_5$ sample, which was 3.6 times higher than the

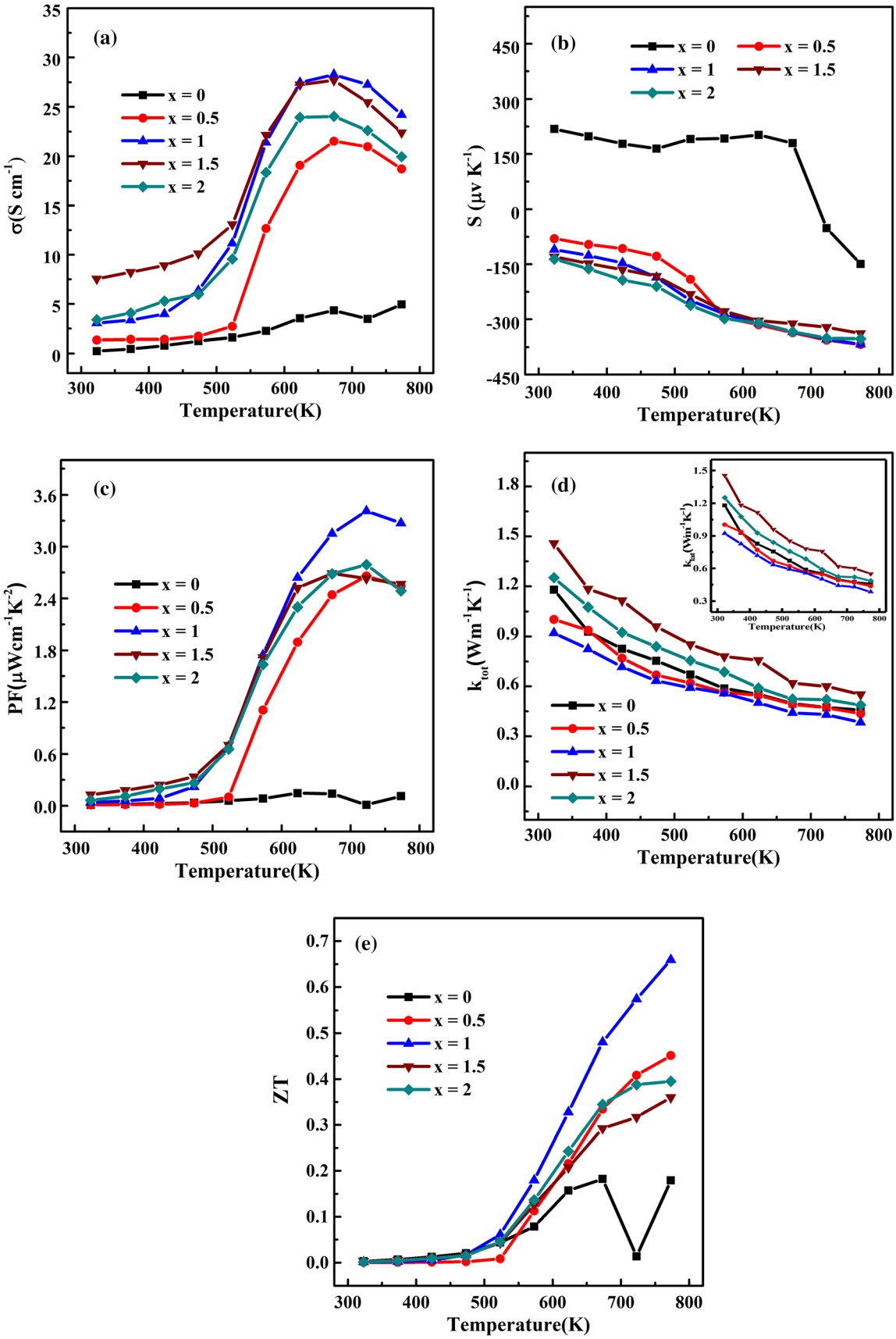

Fig. 3. Temperature dependence of (a) electrical conductivity, (b) Seebeck coefficient, (c) power factor, (d) total thermal conductivity with inset of lattice thermal conductivity and (e) figure of merit ZT for $SnSe_{0.95}$-x%$MoCl_5$ (x = 0, 0.5, 1, 1.5, 2) samples.

Table I. Room temperature Hall carrier concentrations (n_H), mobility (μ) and density (D) of the $SnSe_{0.95}$-x%$MoCl_5$ (x = 0, 0.5, 1, 1.5, 2) samples

x	n_H ($\times 10^{18}$ cm^{-3})	D (g cm^{-3})	μ (cm^2 V^{-1} S^{-1})
0	0.53	5.83	6.91
0.5	5.39	6.02	3.13
1.0	6.24	6.01	5.08
1.5	17.6	6.01	1.65
2.0	2.12	6.00	1.47

undoped SnSe sample (0.18) at 773 K and also higher than the Bi-doped, as previously reported.[10] Although it is still inferior to those of $Sn_{1-x}Re_xSe_{0.93}Cl_{0.02}$ and $Sn_{1.05-x}Pb_xSe_{0.95}Cl_{0.05}$ dual-doped n-type polycrystalline samples,[12,16] this result suggests that $MoCl_5$ is an effective dopant for improving the thermoelectric performances of SnSe using synergistic multipoint-defects strategy.

CONCLUSIONS

In summary, we investigated the thermoelectric properties of polycrystalline $SnSe_{0.95}$-x%$MoCl_5$ (x = 0, 0.5, 1.0, 1.5, and 2) samples fabricated by melting and hot pressing. The doping of $MoCl_5$ enhanced the electrical conductivity due to the increased carrier concentration and reduced the thermal conductivity by introducing the multipoint defects. As a result, the maximum ZT value of 0.66 at 773 K is achieved in $SnSe_{0.95}$-1%$MoCl_5$ along the hot-pressing direction. Our work has illustrated that multipoint defect synergy is effective for tuning carrier concentration and enhancing the thermoelectric performance of n-type SnSe.

ACKNOWLEDGMENTS

This work was sponsored by the Zhejiang Provincial Natural Science Foundation of China (Grant No. LY19E020009).

REFERENCES

1. L.E. Bell, *Science* 321, 1457 (2008).
2. J. He and T.M. Tritt, *Science* 357, eaak9997 (2017).
3. X. Zhang and L.D. Zhao, *J. Materiomics* 1, 92 (2015).
4. L.D. Zhao, C. Chang, G. Tan, and M.G. Kanatzidis, *Energy Environ. Sci.* 9, 3044 (2016).
5. S. Li, Y. Wang, C. Chen, X. Li, W. Xue, X. Wang, Z. Zhang, F. Cao, J. Sui, X. Liu, and Q. Zhang, *Adv. Sci.* 5, 1800598 (2018).
6. L.D. Zhao, S.H. Lo, Y. Zhang, H. Sun, G. Tan, C. Uher, C. Wolverton, V.P. Dravid, and M.G. Kanatzidis, *Nature* 508, 373 (2014).
7. C. Chang, M. Wu, D. He, Y. Pei, C.F. Wu, X. Wu, H. Yu, F. Zhu, K. Wang, Y. Chen, L. Huang, J.F. Li, J. He, and L.D. Zhao, *Science* 360, 778 (2018).
8. Z.G. Chen, X. Shi, L.D. Zhao, and J. Zou, *Prog. Mater Sci.* 97, 283 (2018).
9. Y.K. Lee, Z.Z. Luo, S.P. Cho, M.G. Kanatzidis, and I. Chung, *Joule* 3, 1 (2019).
10. V.Q. Nguyen, T.H. Nguyen, V.T. Duong, J.E. Lee, S.D. Park, J.Y. Song, H.M. Park, A.T. Duong, and S. Cho, *Nanoscale Res. Lett.* 13, 200 (2018).
11. F. Li, W. Wang, X. Qiu, Z. Zheng, P. Fan, J. Luo, and B. Li, *Inorg. Chem. Front.* 4, 1721 (2017).
12. J. Cha, C. Zhou, Y.K. Lee, S.P. Cho, and I. Chung, *ACS Appl. Mater. Interfaces.* 11, 21645 (2019).
13. Q. Zhang, E.K. Chere, J. Sun, F. Cao, K. Dahal, S. Chen, G. Chen, and Z. Ren, *Adv. Energy Mater.* 5, 1500360 (2015).
14. X. Wang, J. Xu, G. Liu, Y. Fu, Z. Liu, X. Tan, H. Shao, H. Jiang, T. Tan, and J. Jiang, *Appl. Phys. Lett.* 108, 083902 (2016).
15. C. Chang, Q. Tan, Y. Pei, Y. Xiao, X. Zhang, Y.X. Chen, L. Zheng, S. Gong, J.F. Li, J. He, and L.D. Zhao, *RSC Adv.* 6, 98216 (2016).
16. Z.H. Ge, Y. Qiu, Y.X. Chen, X. Chong, J. Feng, Z.K. Liu, and J. He, *Adv. Funct. Mater.* 7, 1902893 (2019).
17. S. Romankov, Y. Hayasaka, E. Kasai, and J.M. Yoon, *Surf. Coat. Technol.* 205, 2313 (2010).
18. S. Sassi, C. Candolfi, J.B. Vaney, V. Ohorodniichuk, P. Masschelein, A. Dauscher, and B. Lenoir, *Appl. Phys. Lett.* 104, 212105 (2014).
19. J. Shu, X. Su, H. Xie, G. Zheng, W. Liu, Y. Yan, T. Luo, X. Yang, D. Yang, C. Uher, and X. Tang, *ACS Appl. Mater. Interfaces.* 10, 15793 (2018).
20. S.D. Yang, R.K. Nutor, Z.J. Chen, H.F. Wu, and J.X. Si, *J. Electron. Mater.* 46, 6662 (2017).